A Detailed Look at Vesicle Fusion

A. F. Smeijers,* A. J. Markvoort, K. Pieterse, and P. A. J. Hilbers

Department of Biomedical Engineering, Technische Universiteit Eindhoven, P.O. Box 513, 5600 MB Eindhoven, The Netherlands

Received: February 8, 2006; In Final Form: April 7, 2006

Many different hypotheses on the molecular mechanisms of vesicle fusion exist. Because these mechanisms cannot be readily asserted experimentally, we address the problem by a coarse-grained molecular dynamics simulations study and compare the results with the results of other techniques. The simulations performed include the fusion of small and large vesicles and exocytosis, i.e., the fusion of small vesicles with flat bilayers. We demonstrate that the stalk, the initial contact between two fusing vesicles, is initiated by lipid tails that extend spontaneously. The stalk is revealed to be composed of the contacting monolayers only, yet without hydrophobic voids. Anisotropic and radial expansion of the stalk have been theorized; we show that stalk evolution can proceed via both pathways starting from similar setups and that water triggers the transition from elongated stalk to hemifusion diaphragm.

1. Introduction

The principal function of cell membranes is compartmentalization: each cellular process must be carried out in a specific environment in a controlled way. Vesicular trafficking is the means of directed transport between compartments.[1] Vesicles bud from one organelle and fuse with a target organelle, releasing their contents inside. Similarly, vesicles are utilized in exocytosis.[1] In addition, vesicles find an application as carriers in gene therapy,[2] targeted drug delivery,[3] and contrast enhanced imaging.[4] In this respect, the elucidation of vesicle fusion is of importance. Many in vitro fusion experiments have been performed with liposomes, revealing the fusion dynamics at the millisecond and micrometer scale (e.g., see refs 5 and 6). The basis of vesicle fusion is simple: two vesicles touch and merge to become a single vesicle. The process follows various discrete stages, each relatively easy to discern experimentally. Starting with two vesicles that come into close contact, an initial contact is formed involving lipid mixing of the contacting monolayers, while leaving the contents separated—a stage called hemifusion. Once the vesicle contents mix, full fusion is reached. However, the molecular structures and the transitions between these stages cannot be visualized experimentally with the techniques currently available. With modeling techniques, the fusion process can be studied in more detail. Previous studies used elastic continuum models[7−11] and simulation techniques such as Brownian dynamics,[12] Monte Carlo,[13] dissipative particle dynamics,[14,15] and coarse-grained molecular dynamics (MD).[16,17] Of these techniques, MD is the only one to incorporate solvent explicitly. Here we apply the coarse-grained MD technique to elucidate the fusion of vesicles at the molecular level, and compare the results to theoretical structures.

In theory, the vesicle's inclination to fuse depends on the curvature of the contact zone, and the lipids present. Sonicated vesicles range in size from 21.4 nm[18] to above 1 μm in diameter; their curvatures change accordingly. The lipids influence the fusion process as they generate membrane properties, e.g., through their spontaneous curvature.[19,20]

In fusion models, the contacting monolayers (the external monolayers of the vesicles) are generally labeled cis-monolayers, whereas the inner monolayers are labeled trans-monolayers. The initial lipid connection between the vesicles is widely regarded to be a stalk, a union of cis-monolayers in a toroidal hourglass shape. The original stalk model was envisioned to have the cis-monolayers curved circularly.[7] This and other stalk models are the product of elastic continuum calculations.[21] This method is used to calculate the free energy of hypothetical structures. However, the original stalk model has a substantially higher energy than the bilayers from which it is supposed to stem.[22] The stress-free stalk[8] is a revision of the original stalk. It has gained a lower energy by dropping the assumption of a circular geometry, and by allowing the voids to be filled with lipids of different tail lengths[19] or small hydrophobic molecules. Another revision, the transmembrane contact stalk,[9] is so called because its trans-monolayers make contact at the stalk center; in turn, the monolayers are sharply bent to fill any hydrophobic voids. Recently conducted X-ray diffraction experiments support the existence of stalks.[23] If in this experiment hydrophobic voids are present in the inverted hexagonal phase (as expected[24]), then the images suggest the stalk contains voids as well, although this is not highlighted in the paper.

The stalk model is well received; however, other hemifusion models exist as well. For instance, the extended lipid hemifusion model[25] implies that the cis-monolayers are stacked and joined together by the tails of stretched lipids, while their headgroups stay in the interface.

To explain complete fusion after contact is made, several pathways were conceived. One is the stalk-pore hypothesis.[10] It states that the stalk expands radially, bringing the trans-monolayers together in a transmembrane contact. The contact expands further so a bilayer, called a hemifusion diaphragm (HD), is formed. Because the HD edge is energetically unfavorable, some argue that expansion of the stalk stops before an HD with a radius exceeding the monolayer thickness can be formed,[10] whereas others argue that only large diaphragms exist.[8] Eventually, a fusion pore opens in the HD that is subsequently assimilated. As tensions are concentrated along the rim, that is

* Corresponding author. E-mail: a.f.smeijers@tue.nl.

10.1021/jp060824o CCC: $33.50
Published on Web 05/24/2006

TABLE 1: Overview of Vesicle Fusion Simulations Performed[a]

label	N_{out}	N_{in}	N_w	D_b (nm)	fusion pathway	T_s (ns)	L_s (ns)	L_{hd} (ns)
LARGE1	655	369	3483	1.4	anisotropic, 1 pore	20.6	6.47	34.5
LARGE2	655	369	3497	1.4	anisotropic, 2 pores	0.12	5.47	-
LARGE3	638	380	3555	1.3	radial	8.42	0.96	>86.8
SMALL1	134	26	17	1.7	anisotropic, 1 pore	0.26	2.91	0.24
SMALL2	161	39	66	1.3	anisotropic, 2 pores	8.63	2.02	-
SMALL3	181	58	102	1.5	radial	1.66	1.32	0.26
EXOCY1	181	58	87	1.7	radial	13.3	2.43	0.87
EXOCY2	181	58	87	1.4	anisotropic, 1 pore	5.80	2.65	28.0

[a] The simulations are labeled LARGE for large vesicles, SMALL for small vesicles and EXOCY for "exocytosis" simulations involving small vesicle fusion with a bilayer. For these simulations, the number of lipids in the inner and outer monolayer (N_{in}, N_{out}) and the number of encapsulated water particles (N_w) for each vesicle, the bridging distance (D_b), the fusion pathway, the time to stalk formation (T_s), the stalk lifespan (L_s) and the HD lifespan (L_{hd}) are given. The bridging distance is the intervesicle distance of the configuration before a connection is made.

where the fusion pore is thought to emerge.[10] The fusion pore continues to grow due to reduction of the free edge.[8] In an alternative hypothesis, the direct stalk-pore model,[10,11] the fusion pore directly originates from the radially expanding stalk. In the third hypothesis, the anisotropic stalk-pore model,[12,13] the stalk grows anisotropically, thus forming an elongated connection. Consequently, the stalk destabilizes the bilayers so that holes appear in its vicinity. These holes are then encircled by bending of the stalk, thus a fusion pore is created.

In vitro experiments are used to examine vesicle fusion at a microscopic scale, but on a time scale much larger than the actual lipid dynamics, whereas elastic continuum models consider the fusion intermediates at a submicroscopic scale and do not consider dynamics. Molecular dynamics allows for both, the subnanosecond dynamics being on the scale of individual atoms. To perform simulations of complete vesicle fusion in a reasonable amount of time, we use a coarse-grained approach.

2. Methods

2.1. Model. The coarse-grained model for lipid and water has been presented in a previous paper by Markvoort et al.[26] The coarse-grained lipid is made of four hydrophilic H particles, and two tails of four hydrophobic T particles each. It is based on the glycerophospholipid class of which dipalmitoylphosphatidylcholine (DPPC) is a representative example. The solvent is represented by hydrophilic W particles. All bonded particles in the system are regulated by harmonic bond potentials; the nonbonded interactions are governed by truncated shifted Lennard-Jones potentials. The model was fitted for water and alkanes, instead of lipids in a bilayer, so there is no unnatural bias toward membrane formation. To ensure flexibility of our lipids and to be able to investigate vesicle fusion with relatively small vesicles, no bending potentials are applied.

Due to the smooth potentials and lack of hydrogen bond network, the diffusional time scales of coarse-grained MD simulations are not identical to the time scale implied. One could decide on a calibration factor to make for instance the lateral lipid diffusion a perfect fit. However, in the same system other diffusion coefficients require a different calibration factor, as the factor varies with the mass and size of the particles.[27] Because a general calibration factor for a mixed system does not exist, we have chosen to present the time-dependent results without such a factor.

2.2. Simulations. All simulations described in this paper have been performed at constant temperature (307 K) and constant pressure (1 bar) with time steps of 24 fs and using our in-house developed molecular dynamics code PumMa.[26]

Lipid bilayers were made by randomly distributing a number of lipids in a simulation box filled with water particles. When the simulation is run, a bilayer is formed spontaneously. Pressure scaling was applied independently in all three spatial directions such that no unnatural stress was introduced in the bilayer. Vesicles were made by placing such a bilayer in a larger simulation box. When the simulation is run, the bilayer curls to minimize its edge, ultimately forming a vesicle. This spontaneous bilayer-vesicle transition is entropy driven as shown in ref 26.

The setup for vesicle fusion is made by duplicating the simulation box with the vesicle inside. Both duplications are translated and placed next to each other in a larger simulation box, such that the vesicles start at a relatively small distance from each other; on average 6.3 layers of water particles remain in between. The parts of the box devoid of particles are filled with water. In contrast to the practice of others,[16,17] no restraints are put on the vesicles during the simulations.

3. Results

In the following sections, several fusion simulations are discussed. The simulations consist of either large or small vesicles; the large vesicles have a typical diameter of approximately 17 nm, whereas the small vesicles are typically of size 11 nm in diameter. An overview of the performed simulations and their characteristics is given in Table 1.

3.1. Fusion of Large Vesicles. The first simulation discussed, LARGE1, is one of large vesicles. With large vesicles, the intermediate states of fusion can be visualized properly. This first simulation is treated as a framework for general fusion events that are discussed in detail. Subsequent simulations are treated more concise, focusing on the differences with the events of LARGE1.

3.1.1. Vesicle Movement. In the first simulation (LARGE1) a stalk emerged after 20.6 ns. Before a stalk can be formed, the vesicles have to move into contact range. The intervesicle distance is defined as the minimal distance between the lipids of the two vesicles, measured between the tail particles connected to the headgroup particles. This intervesicle distance is affected by movement of the vesicles on different scales, as shown in Figure 1. The first is caused by Brownian motion. In this case the vesicles drifted toward each other, the centers of mass got about 1.3 nm closer over 20 ns. As the vesicles undulate, this causes an oscillation of the minimal distance on top of the change caused by Brownian motion. The minimum distance was 2.5 nm at the start, it became as high as 3.5 nm and as low as 1.0 nm. At the actual start of stalk formation the vesicles were 1.4 nm apart. The final effect is caused by lipid movement, such as out-of-plane movement, lateral diffusion, and atomic motion. The rapid fluctuation of the intervesicle distance graph is due to this movement.

3.1.2. Stalk Formation. When the vesicles come into close contact, a stalk can be formed. In Figure 2 the formation event

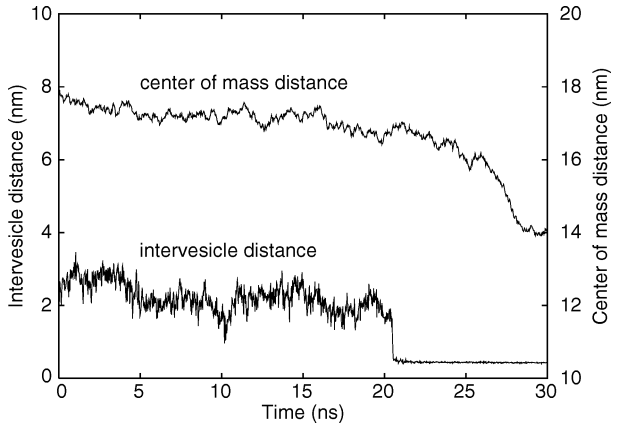

Figure 1. Graph of the intervesicle distance and the distance between the centers of mass of the vesicles' interiors. Evident are vesicle drift, membrane undulations and lipid movement.

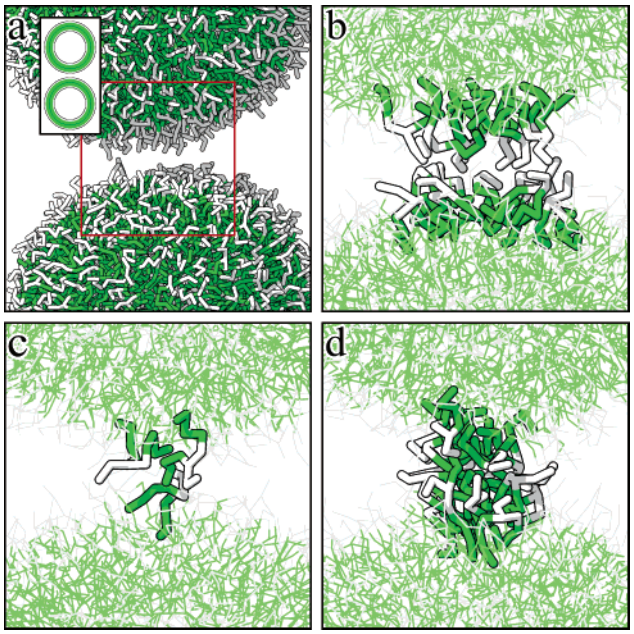

Figure 2. Stalk formation. (b)−(d) show the contact region, highlighted by the red box in (a). In (b)−(d) the view is a cross-section along the vesicle−vesicle axis, as depicted in the inset of (a). This orientation is maintained in all figures unless specified otherwise. Lipids are shown in stick representation with white hydrophilic headgroups and green hydrophobic tails; water has been omitted for clarity. (a) Shortly before fusion commences, the vesicles are at a considerable distance (19.48 ns). (b) The vesicles draw closer and hydrophobic patches appear in both (20.49 ns). (c) Lipid tails form a hydrophobic bridge (20.54 ns). (d) Other lipids complete the stalk (20.61 ns).

is illustrated. First hydrophobic patches emerge on opposite sides of the contact zone (Figure 2b). In these patches the tail ends are at the surface and as their headgroups are out of the way, the tails are less restricted to move into the interstice. Some lipids extend one of their tails into the interstice, bridging the gap between the vesicles (Figure 2c). As these lipids are splayed, this is somewhat reminiscent of extended lipid hemifusion, except for the important fact that the splayed lipids do not interweave the cis-monolayers but rather act as a bridge while the vesicles remain at their respective positions. Clearly the bridging lipids have moved out of the bilayer plane to let their tails connect. Several lipids move along the bridge structure, shielding it from water, thus forming a proper stalk (Figure 2d). From this point on the outer monolayers are connected and their

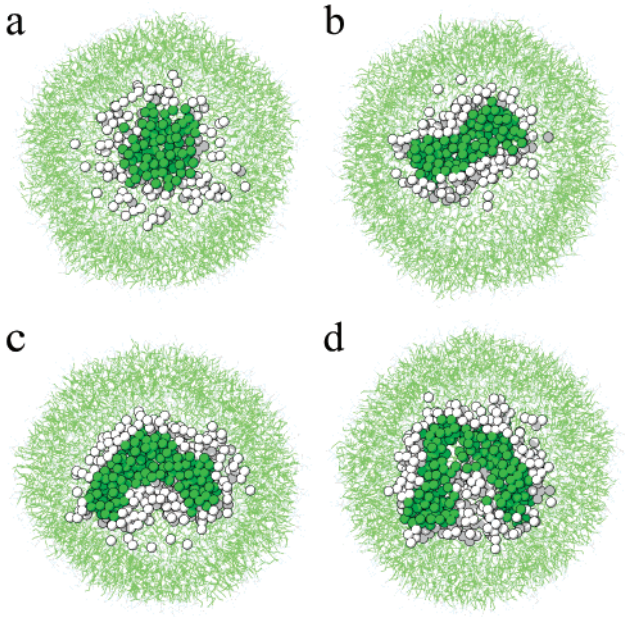

Figure 3. Anisotropic stalk expansion. The view is a cross-section through the stalk region, perpendicular to the vesicle−vesicle axis. The particles lying in the cross-section are shown individually. (a) The initial stalk (20.6 ns). The stalk proceeds to elongate (b) (22.9 ns), and bend (c) (24.7 ns) until it is about to close (d) (26.5 ns).

lipids are allowed to mix. In every fusion simulation we have performed, the stalk never disintegrated once it was formed.

3.1.3. Anisotropic Stalk Expansion. Typically, the stalk is formed where the vesicles are closest together, that is, in the center of the contact zone (Figure 3). In this first simulation, the stalk expands anisotropically into an elongated stalk (Figure 3a,b), which grows and folds to form a ring (Figure 3c,d). In its pocket, the movement of water and lipid headgroups is restricted, but as water can move more freely, it is likely to get out of the pocket first. Visible in Figure 4a is that some water particles manage to slip past the membrane into one of the vesicles. They function as a trigger for pore formation, as several lipid headgroups and water particles follow, thereby opening up the pocket to that vesicle (Figure 4b). Approximately 0.5 ns later, the ring is completed (Figure 4c). In this manner the entire pocket has been internalized into the vesicle (measuring 25 lipids and 35 water particles). The resulting hemifusion diaphragm (Figure 4d) is not a classical one in the sense that it is formed by a single trans-monolayer complemented by the cis-monolayers instead of the other trans-monolayer.

In the second simulation of large vesicle fusion (LARGE2), the stalk-bending mechanism was different in that 0.2 ns after the pocket opened up to one side, it opened up to the other side as well, thereby causing full fusion instantly. Thus anisotropic stalk expansion can lead to stalk-bending with one or two pores, the latter fusion process is markedly faster.

3.1.4. From HD to Full Fusion. The final interesting stage of the fusion process presented by the LARGE1 simulation is the transition from an HD to full fusion. In the hemifused state, the vesicles' interiors are largely the same as in the separated state before fusion, whereas the external surface area is reduced. Hence, the surplus exterior lipids must stretch as they have a smaller area to fill. This results in a substantially thicker external membrane compared to the HD (Figure 5a), which consequently is the weakest part of the structure. Nonetheless, the HD is quite stable; here it took 34.5 ns before a pore emerged near the HD rim. Pore formation is again triggered by the movement of some

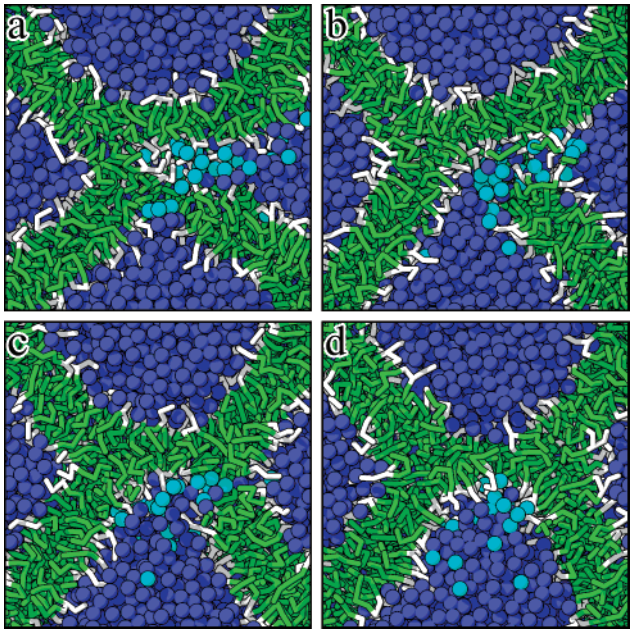

Figure 4. Hemifusion diaphragm formation via stalk-bending and one small pore. Shown is a cross-section along the vesicle−vesicle axis, through the pocket. Water is shown as dark blue van der Waals spheres, and the water particles that enter the bottom vesicle are light blue. (a) Some water enters the vesicle and initializes a pore (26.5 ns). (b) The pore is evident (26.8 ns). (c) As the stalk ring closes and the last water particles enter the vesicle, the pocket is internalized (27.0 ns). (d) A hemifusion diaphragm results (27.2 ns).

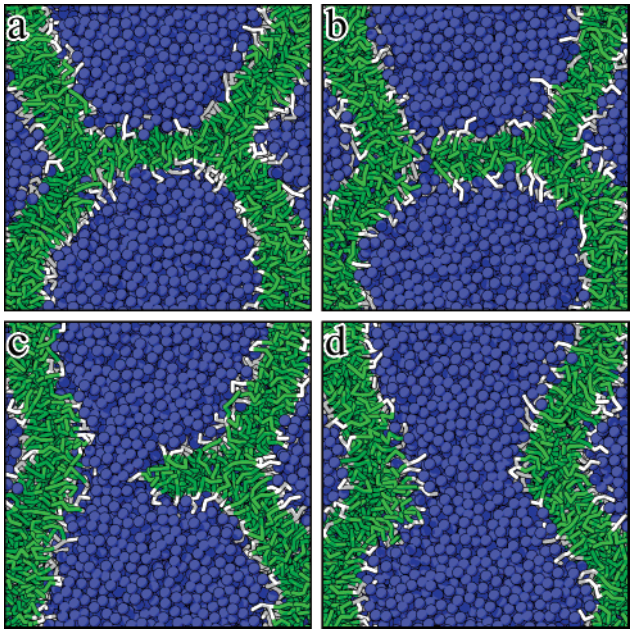

Figure 5. Hemifusion diaphragm breach and assimilation: (a) HD (61.1 ns); (b) HD breach (61.6 ns); (c) HD assimilated as the pore grows (62.4 ns); (d) full fusion (62.8).

water particles across an unstable bilayer (Figure 5b). Had the bilayer been stable, the pore would have quickly receded; instead, the diaphragm contracted to reduce the area per lipid (Figure 5c). Now, in less than 1 ns the HD was assimilated in its entirety (Figure 5d).

With the vesicles fully fused, the lipids and water molecules are again confined to their compartments; there is little water transport and no lipid redistribution over the monolayers. The vesicle as a whole therefore does not become spherical in the remaining 57 ns but instead retains its tubular shape.

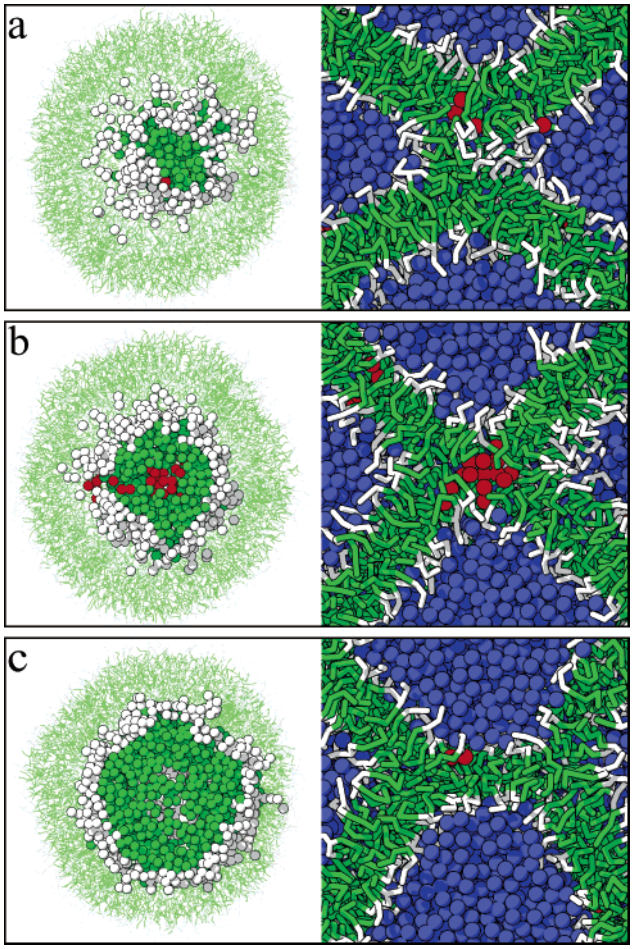

Figure 6. Radial stalk expansion. The left column is a cross-section through the stalk region, perpendicular to the vesicle−vesicle axis; the right column is the normal view along the vesicle−vesicle axis. For clarity, voids are visualized by automatically filling them with additional particles. Note that only clusters of "void particles" indicate substantial voids, whereas solitary "void particles" do not. (a) The stalk is evident (8.7 ns). (b) As the stalk expands radially, a hydrophobic void is present in its center (9.1 ns). (c) When the trans-monolayers connect, a hemifusion diaphragm is formed (9.6 ns).

3.1.5. Radial Stalk Expansion. Whereas the prior two fusion simulations follow the anisotropic stalk expansion path, the third simulation (LARGE3) follows the radial stalk expansion path. This means the cis-monolayers that make up the stalk expand outward, thereby straightening the outer monolayer. As the cis-monolayers expand outward, the contacting part of the monolayers must separate as well, thus leaving an empty space in their wake (Figure 6b). As this void is energetically unfavorable, the mechanism of straightening the outer monolayer now has to compete with the mechanism of reducing void size. Thus, the void size fluctuates, until the inner monolayers plus their contents have changed their shapes to fill the void. Here, the void lasted for 0.5 ns, after which the inner parts of the vesicles have deformed to fill the void and form an HD (Figure 6c). In the case of large vesicles, radial stalk expansion is considerably faster than anisotropic stalk expansion. Here within 1 ns after the appearance of the stalk an HD is already formed.

Although the LARGE3 simulation has been continued for almost 90 ns after HD formation, a fusion pore has not appeared in the HD—it is still expected to, however, as it took a long time in LARGE1 as well. However, a control simulation was performed starting with a configuration of LARGE3 in which the stalk expanded radially, with a minute difference in particle

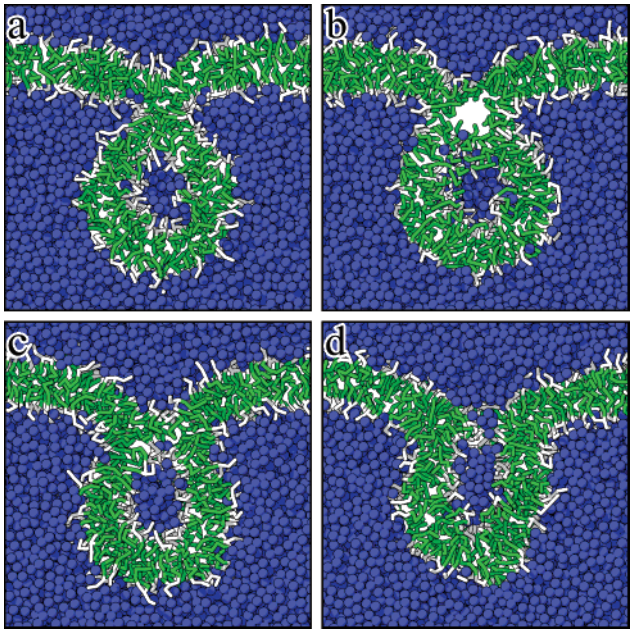

Figure 7. Thin slices through the center of a small vesicle fusing with a bilayer. (a) The stalk is formed (15.4 ns). (b) It expands radially, so a hydrophobic void is present (15.6 ns). (c) A small HD is formed by adaptation of the trans-monolayers (15.7 ns). (d) Then a pore opens up the HD (16.5 ns), and the water content of the vesicle is released across the bilayer.

velocities. In this simulation, the stalk expands normally, but almost immediately after HD formation, it is already punctured. Thus, this small HD lasted for only 0.22 ns.

3.2. Fusion of Small Vesicles. The fusion process has also been studied for smaller vesicles. In the first simulation (SMALL1) the vesicles fuse according to the anisotropic stalk expansion model. A single pore is formed, thus an HD state follows, which is short-lived. In the second simulation (SMALL2) the anisotropic stalk expansion pathway is followed as well, but here two pores are formed, thus the second hemifusion state is bypassed. In the third simulation (SMALL3) the vesicles fuse according to the radial stalk expansion principle. This includes the presence of a transient void. As the inner parts of the vesicles are deformed to fill the void, a short-lived HD is formed. After only 0.12 ns the HD opens when lipid heads and water from both vesicles make contact. During the remainder of all three simulations the vesicles retain an elongated shape. Small vesicle fusion thus follows the general pathways of the large vesicle fusion simulations, providing a fast alternative to study the process.

3.3. Exocytosis: Fusion of Vesicle and Bilayer. In all previous simulations both vesicles were of equal size. In nature, this is usually not the case. In the process of exocytosis, for example, material is discharged from the cell via fusion of a vesicle with the much larger cell membrane.[1] To model exocytosis, we focus on the contact zone between vesicle and cell membrane. Due to differences in size, the cell membrane is modeled as a flat bilayer. In the first simulation a small vesicle and a bilayer of 904 lipids are considered. As the curvature of a bilayer is minute, especially compared to the curvature of small vesicles, it is of interest to investigate whether their combination differs from the fusion process described above.

In the first exocytosis simulation (EXOCY1), a stalk formed after 13.3 ns (Figure 7a). Stalk formation is normal as the bridging lipids come from both monolayers. The stalk has a tendency to elongate, but little room was available in the contact zone for stalk-bending. Eventually, the concave monolayer was released from the convex monolayer, leaving a hydrophobic void (Figure 7b). The void was mainly filled by the distal monolayer of the bilayer and somewhat by deformation of the vesicle interior; the bilayer looks cratered as a result (Figure 7c). The curved nature of the hemifusion state imposes a strain on the waist that can be relieved by straightening the membrane. This force pulls at the HD; thus a pore opened up in the center of the HD (Figure 7d), and the vesicle contents are released.

In the second exocytosis simulation (EXOCY2), with slightly different initial particle velocities, the stalk followed the anisotropic stalk expansion scenario. The HD lasted much longer than in the previous simulation (28.0 ns versus 0.8 ns) and thus had the time to grow larger as well (on average 18 nm^2.) A fusion pore was initiated by water crossing the diaphragm membrane, thus completing the fusion process.

The fusion mechanisms of these simulations are qualitatively similar to the vesicle fusion simulations described above.

4. Discussion

In this section the various stages of fusion, as observed in our simulations, are compared to the various hypotheses presented in the Introduction. Additionally, the characteristics of the two modes of stalk expansion are distinguished.

4.1. Bridging Lipids. We demonstrated the spontaneous formation of a stalk, initiated by splayed lipids forming a bridge structure. Such a transient structure of single lipids was not and cannot be described by elastic continuum models. By using a coarse-grained model, the details of stalk formation can be observed, but what initiates stalk formation? Here explanations are suggested on the basis of these observations.

Apparently, the bridging lipids originate from hydrophobic patches. There is no immediate explanation as to why these patches emerge. The attraction between hydrophilic particles is identical for water and headgroup particles; there is no reason headgroups would preferentially aggregate. However, without a preferred state the system fluctuates between states, thus occasionally sizable hydrophobic patches are present. The appearance of hydrophobic patches does not require imminent fusion.

The position of the lipids that initiate the bridge in these hydrophobic patches is such that one of their tails is folded back toward the headgroup region, but not yet extended into the solvent. Even regular isolated bilayers or vesicles have some amount of backfolded lipids, not limited to hydrophobic patches. In our model bilayers, on average 11% of the lipid tail ends are folded back, 4.7% are near water and thus part of a patch with minimal water shielding. These percentages rise with increasing curvature. For the outer monolayer of the large vesicle (LARGE1) 15% of the lipid tails are backfolded, 8.8% are accessible to water. For a small vesicle (SMALL3) these values are 19% and 12%, respectively. These findings support the notion that stalk formation is easier for smaller vesicles.

Although the flexibility of our model lipids does make backfolding less costly, it is not limited to our model; e.g., it is also found in a united atoms model[28] where 2% of the lipids in a flat bilayer have an alkyl chain outside the average plane and in other coarse-grained vesicles.[29] Furthermore, it should be stressed that these backfolded lipids are not in the extended conformation: the lipids are not stretched and their tails are not in the water phase. In fact, in all the bilayer simulations we have performed, a lipid was never found to be in the extended conformation of stable bilayers as suggested,[25,30] although the flexibility of our lipids surely would have permitted it.

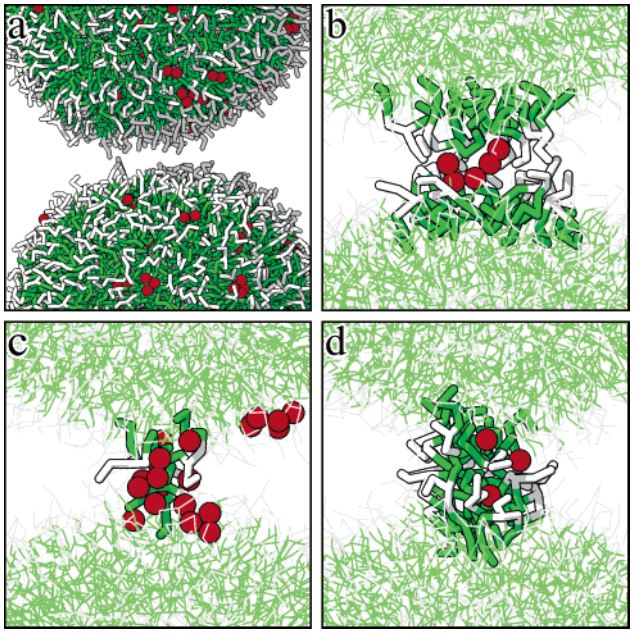

Figure 8. Stalk formation, the images of Figure 2 repeated with added particles filling and thereby highlighting the voids: (a) vesicles (19.48); (b) hydrophobic patches (20.49 ns); (c) hydrophobic bridge (20.54 ns); (d) stalk (20.61 ns).

Among other things, Table 1 lists the bridging distance, the distance lipid tails need to span to serve as basis for the stalk. This intervesicle distance ranges from 1.3 to 1.7 nm. This is consistent with GUV fusion experiments, where a reduction of intervesicle distance from 3 to 1 nm was found to trigger (hemi)-fusion.[5] However, this distance is beyond the cutoff radius of the Lennard-Jones potential between two T particles. Therefore, the T particles of opposite vesicles are not able to sense each other before fusion. Furthermore, achieving the bridging distance is not sufficient to initiate a lipid bridge. In the simulations, often the bridging distance was reached various times before the stalk actually formed. For instance in LARGE1 the bridging distance of 1.4 nm was reached at least seven times earlier; once the distance was no more than 1.0 nm (Figure 1). Thus the question remains, what triggers lipid bridging?

On closer inspection, another mechanism becomes apparent. Namely, small voids in the water phase accompany the lipids that are forming the bridge between vesicles in the simulations (Figure 8). These voids facilitate bridge building, they are empty spaces whose presence allows some lipids to extend their tails without energy gain repercussions. How these voids come to be may be for entropic reasons. A thin water layer is entropically unfavorable, so the water in the cleft moves aside to the bulk, thus facilitating tail movement. As water and lipid tail particles associate with like particles, the process is self-amplifying; a moving lipid tail instigates a void through which it can move.

We have shown that vesicles can fuse spontaneously and the stalk forms in the center of the contact zone, as the lipid bridge forms spontaneously between vesicles at a small but considerable distance. This contradicts with the work of Stevens et al.,[17] who, using a similar CG model, conclude that stalks emerge at the edge of the contact zone. However, this is based on the assumption that spontaneous vesicle fusion requires excessive simulation time. Consequently, their simulations are geared toward rapid fusion: the vesicles are constructed by placing lipids on a spherical template, their interior is put under pressure and extra forces are applied to all vesicle particles. With these extra forces the stressed vesicles are pushed together. In the resultant configuration of flattened vesicles, multiple stalks emerge at the strained edge of the contact zone.

4.2. Stalk. When the bridging lipids are joined by others, a stalk is the result. In all our simulations, the stalk has an identical structure, but how does this structure relate to the various stalk models defined through the elastic continuum theory? The models can be differentiated by the shape of the trans-monolayers (from flat to bent), the accompanying void in the bifurcation, and the associated lipid tilt and splay.

In the simulations, there are no hydrophobic voids present in the membrane core during the transition from separated vesicles to vesicles connected by a stalk. The stalk forming process is sufficiently slow and the lipids are sufficiently flexible to allow the lipid tails to remain connected. The lack of voids is in agreement with the transmembrane contact stalk, except that in our case the trans-monolayers do not make contact and are only moderately bent. In this respect, the stress-free stalk model better resembles the simulation stalks, despite that they are voidless. Thus we propose a stalk structure closely resembling the stress-free stalk, but without hydrophobic voids; they are "filled" with lipids undergoing tilt and splay.

4.3. Anisotropic Stalk Expansion and Stalk-Bending. When, of the two pathways leading to full fusion, the pathway of stalk elongation and bending is followed, a small transient pore emerges in the pocket formed by the bent stalk. The pore allows the uptake of lipids and water from the cavity. The question whether pore formation is triggered by a trace of water through the membrane, or the pore is only the result of a stressed membrane, is addressed here. To provide insight, a simulation has been performed. As a starting-point, the configuration of LARGE1 at 0.04 ns before water pore emergence has been taken, and all water particles have been removed from the cavity. The resulting events are the same, except that indeed the water pore is initiated later (0.41 vs 0.04 ns) as the cavity has to be refilled with water particles before pore formation can be triggered. A transient pore could also be formed by lipids solely, but apparently the energy barrier cannot be overcome without water involvement.

Our simulations support the stalk-bending hypothesis presented in the Introduction fairly well. The fact that the stalk may elongate and bend is in agreement with the model. Furthermore, the case in which two pores are formed and the hemifusion diaphragm is bypassed, is almost entirely analogous. The case where only one pore is formed suggests a major revision, as the hypothesis does not entail the formation of a HD. Another difference is the manner in which the pores appear. In our simulations the pores always appear in the cavity of the bent stalk, the hypothesis suggests pore formation in the general vicinity of the stalk, followed by enveloping of these pores. Thus, the simulations demonstrate a more ordered mechanism than the hypothesis suggest. This difference is due to the methods used. The Brownian dynamics simulations, with which the anisotropic stalk effect was first demonstrated,[12] do not reproduce hydrodynamic behavior[31] and utilize small rod-shaped lipids, thus creating unstable vesicles and promoting disordered fusion.

4.4. Radial Stalk Expansion. During the transition from radially expanded stalk to hemifusion diaphragm a fairly large void appears. At first glance this might seem incorrect, but it is not as improbable as it may seem. A void is merely an absence of matter, an empty space. A void collapses rapidly because neighboring particles have a greater chance to move into a void than into a mass of other particles, simply because there is nothing to stop them. Granted, a void is not a preferential state.

Particles preferably are in the vicinity of particles of the same kind. However, because the mutual attraction of hydrophobic particles is lower than the attraction of hydrophilic particles—they have a lower well depth in the Lennard-Jones potential—it is expected that the tails separate rather than the headgroups separate from water. Indeed, the monolayer attachment is the weakest interaction of the membrane. For instance, with the freeze−fracture technique, membranes are often split in two monolayers. Furthermore, despite the shortcomings in Brownian dynamics simulations, the appearance of a void during this transition is reported by Noguchi et al.[12] as well.

4.5. Radial or Anisotropical Stalk Expansion. The stalk can expand radially or anisotropically, but what are the characteristic differences that make a stalk expand radially or anisotropically? Both transitions from stalk to (hemi)fusion have different characteristics. For instance, the amount of lipids occupied in the bent stalk is larger than in the radial expanded stalk. These lipids are extracted from the cis-monolayers, so these must have spare lipids to build an elongated stalk. In this sense, spare lipids are lipids that are not required to shield the trans-monolayers, which depends on the ability of the lipids to flatten and shield a larger area. However, predicting the number of spare lipids is not straightforward. For instance, a simulation of the fusion of two flat bilayers shows that even with the same amount of lipids on cis- and trans-monolayers, lipids can be spared to construct a large elongated stalk. Moreover, bilayer fusion does not go beyond the elongated stalk phase. The stalk elongates and bends but is not steered toward a tight ring that would lead to pore formation. This shows that the shape of the elongated stalk depends on the shape of the contact zone. Whereas a radially expanded stalk would require fewer lipids than a long elongated stalk, there is no immediate gain in expanding radially. On the contrary, radial expansion is accompanied by a transient hydrophobic void. In the small vesicle simulations, this energetically unfavorable phase is readily compensated by reducing bending tension by complete flattening of the outer monolayer—a cylinder shape is preferred over an hourglass-shape. Regardless of the preferences caused by curvature, even if the amount of spare lipids could be calculated and the contact zone mapped, it would still be impossible to predict beforehand which pathway fusion would take. In particular, similar setups (e.g., the exocytosis simulations) evolve via different pathways, showing that subtle differences have major consequences.

4.6. Hemifusion Diaphragm. After radial stalk expansion and anisotropic stalk expansion with a single pore, a hemifusion diaphragm develops. The size of the HD surface area is controlled by two opposing mechanisms of the external monolayer. One is minimization of bending tension by flattening of the monolayer, the other is minimization of tension caused by overcrowding. Due to the reduced exterior area because of hemifusion, each external lipid must cover a smaller area, which causes tension. In the LARGE1 simulation this causes the HD size to fluctuate around 38 nm^2 with amplitude of about 6 nm^2. When, in a control simulation, 15% of the exterior lipids were removed, thereby reducing monolayer overcrowding tension, the HD grew to 65 nm^2. This means that in the anisotropic stalk expansion scenario, the involvement of the transient pore in HD formation is 2-fold. On one hand it triggers HD formation, on the other hand it redistributes lipids and water so the HD can grow larger than would be possible otherwise.

Of the fusion hypotheses only the stalk pore hypothesis recognizes a sizable hemifusion diaphragm structure. However, there is no consensus on the size an HD can adopt, although it is agreed that small diaphragms are energetically unfavorable. Some insist that the diameter cannot exceed the thickness of a bilayer,[10] whereas others claim that HDs grow to overcome this constraint.[8] The simulations are in accordance with both viewpoints, the HD either ruptures almost immediately or grows as much as possible—only limited by the compressibility of the outer monolayer—and is stable for quite a long time.

5. Conclusion

Vesicle fusion is essentially a mechanism of lipid rearrangement. We have used coarse-grained molecular dynamics to monitor these vast rearrangements over a relatively long time span. We have performed spontaneous unbiased fusion experiments with vesicles ranging between 160 and 1024 lipids, and with combinations of bilayers and small vesicles. In all simulations, the fusion process is analogous, but the stalk evolution may differ. From Table 1 it is clear that whether the fusion process follows the radial stalk expansion route or the stalk-bending route is not solely a matter of vesicle size, bridging distance, or acclimatization time. For large vesicles radial stalk expansion is considerably faster than stalk-bending, although the latter is more frequent. Typically, small vesicles fuse faster than large vesicles. They have a high curvature, so their lipids' tails are quite exposed to water and have much freedom of movement. The simulations of exocytosis show that a vesicle can fully fuse with a bilayer, but only if it is small enough to warrant radial stalk expansion or restricted stalk-bending, because two flat fusing bilayers do not overcome the anisotropically expanded stalk state. Generally, the preference for a fusion pathway varies with decreasing curvature at the contact area. Small vesicles develop a radially expanded stalk—reduction of monolayer curvature is a strong driving force here—or a bent stalk if the contact area permits. When the curvature decreases, the contact zone becomes too large to direct an elongated stalk into a tight ring, and the vesicles remain in a hemifused state. The fusion process is thus characterized by rapid transitions between long periods of stability. These transitions are initiated by trigger events that each have a small chance of happening; transitions that can nicely be shown using coarse-grained simulations.

References and Notes

(1) Alberts, B.; Bray, D.; Lewis, J.; Raff, M.; Roberts, K.; Watson, J. D. *Molecular biology of the cell*; Garland: New York, 1994.
(2) Audouy, S. A. L.; de Leij, L. F. M. H.; Hoekstra, D.; Molema, G. *Pharm. Res.* **2002**, *19*, 1599−1605.
(3) Fattal, E.; Couvreur, P.; Dubernet, C. *Adv. Drug Delivery Rev.* **2004**, *56*, 931−946.
(4) Mulder, W. J.; Strijkers, G. J.; Griffioen, A. W.; van Bloois, L.; Molema, G.; Storm, G.; Koning G. A.; Nicolay, K. *Bioconjugate Chem.* **2004**, *15*, 799−806.
(5) Heuvingh, J.; Pincet, F.; Cribier, S. *Eur. Phys. J. E* **2004**, *14*, 269−276.
(6) Lei, G.; MacDonald, R. C. *Biophys. J.* **2003**, *85*, 1585−1599.
(7) Kozlov, M. M.; Markin, V. S. *Biofizika* **1983**, *28*, 242−247.
(8) Markin, V. S.; Albanesi, J. P. *Biophys. J.* **2002**, *82*, 693−712.
(9) Kozlovsky, Y.; Kozlov, M. M. *Biophys. J.* **2002**, *82*, 882−895.
(10) Kozlovsky, Y.; Chernomordik, L. V.; Kozlov, M. M. *Biophys. J.* **2002**, *83*, 2634−2651.
(11) Kuzmin, P. I.; Zimmerberg, J.; Chizmadzhev, Y. A.; Cohen, F. S. *Proc. Natl. Acad. Sci. U.S.A.* **2001**, *98*, 7235−7240.
(12) Noguchi, H.; Takasu, M. *J. Chem. Phys.* **2001**, *115*, 9547−9551.
(13) Müller, M.; Katsov, K.; Schick, M. *J. Chem. Phys.* **2002**, *116*, 2342−2345.
(14) Li, D.-W.; Liu, X. Y. *J. Chem. Phys.* **2005**, *122*, 174909.
(15) Shillcock, J.; Lipowsky, R. *Nat. Mater.* **2005**, *4*, 225−228.
(16) Marrink, S. J.; Mark, A. E. *J. Am. Chem. Soc.* **2003**, *125*, 11144−11145.
(17) Stevens, M. J.; Hoh, J. H.; Woolf, T. B. *Phys. Rev. Lett.* **2003**, *91*, 188102.

(18) Cornell, B. A.; Fletcher, G. C.; Middlehurst, J.; Separovic, F. *Biochim. Biophys. Acta* **1982**, *690*, 15−19.
(19) Haque, M. E.; Lentz, B. R. *Biochemistry* **2004**, *43*, 3507−3517.
(20) Zimmerberg, J. *Traffic* **2000**, *1*, 366−368.
(21) Helfrich, W. *Z. Naturforsch., C: Biosci.* **1973**, *28*, 693−703.
(22) Lentz, B. R.; Siegel, D. P.; Malinin, V. *Biophys. J.* **2002**, *82*, 555−557.
(23) Yang, L.; Huang, H. W. *Science* **2002**, *297*, 1877−1879.
(24) Turner, D. C.; Gruner, S. M. *Biochemistry* **1992**, *31*, 1340−1355.
(25) Kinnunen, P. K. J.; Holopainen, J. M. *Biosci. Rep.* **2000**, *20*, 465−482.
(26) Markvoort, A. J.; Pieterse, K.; Steijaart, M. N.; Spijker, P.; Hilbers, P. A. J. *J. Phys. Chem. B* **2005**, *109*, 22649−22654.
(27) Nielsen, S. O.; Lopez, C. F.; Srinivas, G.; Klein, M. L. *J. Phys.: Condens. Matter* **2004**, *16*, R481−R512.
(28) Ohta-Iino, S.; Pasenkiewicz-Gierula, M.; Takaoka, Y.; Miyagawa, H.; Kitamura, K.; Kusumi, A. *Biophys. J.* **2001**, *81*, 217−224.
(29) Marrink, S. J.; Mark, A. E. *J. Am. Chem. Soc.* **2003**, *125*, 15233−15242.
(30) Corkery, R. W. *Colloids Surf., B* **2002**, *26*, 3−20.
(31) Frenkel, D.; Smit, B., Eds. *Understanding molecular simulation*; Academic Press: New York, 2002.